Journal of Thermal Analysis and Calorimetry, Vol. 87 (2007) 2, 417–422

ACID PROPERTIES OF SEMICRYSTALLINE ZEOLITIC MESOPOROUS UL-ZSM-5 MATERIALS

A. Ungureanu[1,2], *H. V. Thang*[1], *D. Trong On*[1], *E. Dumitriu*[2] *and S. Kaliaguine*[1*]

[1]Department of Chemical Engineering, Laval University, Ste Foy, Québec G1K 7P4, Canada
[2]Laboratory of Catalysis, Technical University of Iasi, 71 D. Mangeron, 6600 Iasi, Romania

UL-ZSM-5 materials have been prepared by templated solid-state crystallization of zeolites starting from the amorphous mesostructured aluminosilicate Al-Meso. Microcalorimetry and FTIR have been employed to characterize their surface acidity. In good agreement with ^{27}Al MAS NMR data, UL-ZSM-5 displayed an improved density and strength of Brönsted acid sites, as compared to Al-Meso, owing to the incorporation of aluminium in a tetrahedral environment similar to that of zeolite ZSM-5. Moreover, they showed an enhanced Brönsted/Lewis relative acid ratio. However, Al-Meso showed the highest concentration of strong Lewis acid sites due to its largest amount of aluminium in extraframework positions.

Keywords: *acidity, FTIR, mesoporous molecular sieves, microcalorimetry, UL-zeolites, zeolites*

Introduction

The development of mesostructured aluminosilicates with zeolite-like connectivity in their framework is of great interest in the area of catalysis [1–3]. It has been reported that these materials showed an improved acidity and hydrothermal stability, as compared to conventional mesostructured aluminosilicates, due to the induced zeolite order into their amorphous pore walls. Additionally, they retain the advantage of mesostructured materials, overcoming the space constraints of zeolites and allowing thus the diffusion and conversion of bulky organics [1, 2]. The number of works dealing with the development of such materials containing both micropores and mesopores has grown rapidly and promising synthesis approaches have been proposed. They encompass the simultaneous or sequential synthesis of zeolite/mesostructured composite materials [4–6], the autoassembly of protozeolitic nanoclusters (also known as zeolite seeds) under various conditions that generally afford hexagonal mesostructures [7–11], as well as the replication of mesostructured aluminosilicates from mesoporous carbons and by using zeolite precursors [12]. Recently, two novel approaches for synthesizing mesostructured materials with zeolite-like characteristics have been reported by our laboratory. The first one generally deals with the coating of zeolite nanoclusters on the surface of mesostructured materials [13–16]. The second one, which yields materials denoted as UL-zeolites, is based on the templated secondary solid state crystallization of a nanozeolite phase from the amorphous walls of a mesostructured aluminosilicate precursor [17, 18].

In a previous work, we investigated by nitrogen adsorption, XRD and TEM, the effect of crystallization time on the physico-chemical properties of UL-ZSM-5 materials (Si/Al=100) [17]. It has been reported that the amorphous walls of a mesostructured aluminosilicate precursor are progressively transformed into nanocrystalline microporous zeolitic ZSM-5 domains (10–30 nm in size for UL-ZSM-5 after 5 days of crystallization). The acidity of these materials was determined by FTIR of adsorbed pyridine, the results showing indeed that the number and strength of Brönsted acid sites is highly improved as compared to the mesostructured aluminosilicate precursor. Moreover, UL-ZSM-5 materials showed improved hydrothermal stability [18]. In this respect, this paper reports on the characterization of the acidity of semicrystalline zeolitic mesoporous UL-ZSM-5 materials having a Si/Al ratio of about 50 by using NH_3 adsorption microcalorimetry and FTIR of adsorbed pyridine. Additionally, ^{27}Al MAS NMR was used to characterize the coordination state of aluminium in UL-ZSM-5. The acid properties have been compared with those of two reference samples having similar aluminium content that are the amorphous mesostructured aluminosilicate precursor and a fully crystalline ZSM-5 zeolite respectively.

* Author for correspondence: serge.kaliaguine@gch.ulaval.ca

1388–6150/$20.00

Akadémiai Kiadó, Budapest, Hungary
Springer, Dordrecht, The Netherlands

Experimental

Two samples of UL-ZSM-5 were prepared by a secondary templated solid state crystallization of zeolites (0–4 days of crystallization) starting from an amorphous mesostructured aluminosilicate with wormhole-like structure (designated as Al-Meso), as previously reported [17].

In the first step, Al-Meso was prepared by using $SiCl_4$ and $AlCl_3$ as silicon and aluminium sources respectively and poly(alkylene oxide) triblock copolymer (Pluronic P-123, BASF) in ethanol as surfactant, as reported in reference [19]. In the second step, the surfactant containing Al-Meso was impregnated with an aqueous solution of 10% tetrapropylammonium hydroxide (TPAOH) followed by ageing at room temperature. The obtained dried power was introduced into a Teflon-lined autoclave and crystallization has been carried out at 403 K for 2 and 4 days respectively. The final materials were washed with distilled water, dried at 373 K and calcined at 823 K for 6 h. The samples are designated as UL-ZSM-5-*x* where *x* stands for the crystallization time in days. A zeolite ZSM-5 sample was also prepared according to reference [20].

Solid state ^{27}Al MAS NMR spectra were recorded for the calcined samples at room temperature using a Bruker ASX 300 spectrometer.

The differential heat of adsorption of NH_3 were determined using a heat-flow microcalorimeter of the Tian-Calvet type (Setaram C80) equipped with an injection system that allows the feeding of successive doses of NH_3 gas. Prior to adsorption experiments, 50 mg of the sample was evacuated at 673 K overnight under high vacuum ($2 \cdot 10^{-5}$ mbar) using a turbo-molecular pump (Leybold). The equilibrium pressure after each adsorption step was measured by means of a differential pressure gauge (Leybold). Successive gas pulses were sent onto the sample until a final equilibrium pressure of ~1.1 torr was attained. The adsorption has been made at a temperature of 353 K.

The FTIR spectra of adsorbed pyridine over self-supporting wafers were collected at room temperature on a Biorad FTS-60 spectrometer. Wafers of 10 mg cm^{-2} were obtained by compressing solid samples for one minute (6000 lb force) and introduced in a specially designed cell with CaF_2 windows. Prior to pyridine adsorption, the wafers were evacuated overnight at 673 K under high vacuum. Pyridine adsorption was performed at room temperature until saturation (15 min). Pyridine desorption was made stepwise at different temperatures. The Brönsted/Lewis ratio was calculated from IR spectra after desorption of pyridine at 423 K using the molar extinction coefficients determined by Emeis [21].

Results and discussion

UL-ZSM-5 and the reference samples were first characterized by N_2 adsorption, XRD, FTIR. For sake of brevity, only the physico-chemical aspects relevant to acidity characterization will be discussed bellow in a detailed fashion. The physico-chemical properties are reported in Table 1. The results show that the total surface area (S_{BET}), which is high for Al-Meso, decreases from 800 to 430 $m^2\ g^{-1}$ for UL-ZSM-5 after 4 days of crystallization. However, the micropore volume increases as the crystallization time increases. For example UL-ZSM-5-4 displays a micropore volume of 0.149 $cm^3\ g^{-1}$. Note that micropore volume in the case of ZSM-5 is 0.15 $cm^3\ g^{-1}$. The solid state crystallization was followed by an increase in the mesopore radius as well as in the mesopore volume. N_2 adsorption/desorption isotherms of UL-ZSM-5 are of IUPAC type IV with H_1 hysteresis loop and steep rise at low values of relative pressure, indicating the dual pore system (microporous and mesoporous). UL-ZSM-5 samples displayed diffraction patterns in the 22.5-25.5° 2θ range, consistent with ZSM-5, while Al-Meso showed no diffraction patterns above 10° which is indicative of its amorphous pore walls. Furthermore, the crystallinity (see Table 1) increases with the time of crystallization, reaching 65% for UL-ZSM-5 after 4 days of crystallisation. This confirms the progressive change of amorphous walls of Al-Meso into crystalline ZSM-5 nanoparticles. FTIR analyses further suggest the presence of ZSM-5 phase in UL-ZSM-5 samples. The FTIR spectra of both UL-ZSM-5 and ZSM-5 show bands at ~550 cm^{-1}

Table 1 Physico-chemical properties of the aluminosilicate samples

Material	Si/Al[a]	S_{BET}/ $m^2\ g^{-1}$	Micro vol./ $cm^3\ g^{-1}$	Meso vol./ $cm^3\ g^{-1}$	Meso radius/ Å	Crystallinity/ %
Al-Meso	51	800	–	0.859	30	–
UL-ZSM-5-2	43	580	0.142	1.202	130	30
UL-ZSM-5-4	44	430	0.149	2.162	190	65
ZSM-5	58	420	0.150	–	–	100

[a]Si/Al ratio determined by AAS

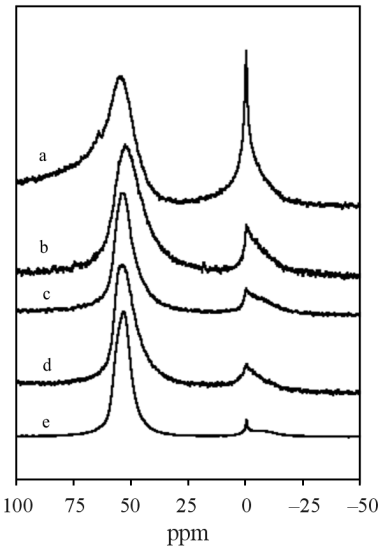

Fig. 1 ^{27}Al MAS NMR spectra of calcined samples of a – Al-Meso, b – UL-ZSM-5-0, c – UL-ZSM-5-2, d – UL-ZSM-5-4 and e – ZSM-5

characteristic of the asymmetric stretching mode of the five-membered rings in pentasil-type zeolites, whereas the spectrum of Al-Meso lacked this band. Moreover, the intensity of this band increased with the time of crystallization.

Figure 1 shows the ^{27}Al MAS NMR spectra of UL-ZSM-5 as well as the reference samples. All the spectra show two main resonances around 53 and 0 ppm which can be assigned to the chemical shifts of tetrahedrally coordinated aluminium in the framework (Al IV) and octahedrally coordinated extraframework (Al VI) respectively [22, 23]. The spectrum of calcined Al-Meso (curve a) shows the part of aluminium atoms tetrahedrally coordinated. A very intense resonance at 0 ppm can be observed, clearly indicating a large amount of octahedral aluminium in extraframework position. Furthermore, the peak at 53 ppm is broad, which results from the presence of aluminium in an environment with a low symmetry, characteristic of amorphous aluminosilicates [16, 24]. The spectrum of UL-ZSM-5 sample before crystallization (curve b) displays also a broad peak at 53 ppm, whereas a reduced amount of Al VI can be noted, as compared to Al-Meso. For UL-ZSM-5 samples after crystallization for 2 and 4 days respectively (curves c and d), the spectra show however peaks at 53 ppm similar in sharpness to that of ZSM-5 (curve e) and a low intensity of the peak at 0 ppm. These results strongly suggest that the environment of the largest part of aluminium atoms in semi-crystalline UL-ZSM-5 is very similar to that of fully crystalline ZSM-5, whereas that of Al-Meso is characteristic of amorphous aluminosilicates. The framework/extraframework aluminium relative ratio increases therefore with the crystallinity of the samples in the order: Al-Meso<UL-ZSM-5-2~UL-ZSM-5-4<ZSM-5.

Heat flow microcalorimetry, which combines the equilibrium adsorption of ammonia and calorimetric measurements of the differential heat of adsorption on the surface of the aluminosilicate samples, is a useful technique to determine the number and strength of acid sites [25, 26]. Therefore, the effect of crystallinity on the surface acidic properties of the UL-ZSM-5 samples was investigated. Figure 2 shows the volumetric isotherms of NH_3 adsorption equilibrium at 353 K. For ZSM-5, in the low-pressure range up to about 0.02 Torr, the amount of NH_3 adsorbed increases quickly with pressure and the initial isotherm region is almost vertical (isotherm d). This can be associated with the acid sites of zeolite ZSM-5 that give very strong interactions with NH_3 molecules. Contrarily, the corresponding initial rise in NH_3 coverage on Al-Meso (curve a) is less steep, the maximum coverage not surpassing 0.1 μmol m^{-2}. This is the result of the low surface acidity of the mesostructured aluminosilicate Al-Meso. Similar values for the coverage of NH_3 at low pressure have been reported for H–Al-MCM-41 [27]. For UL-ZSM-5-2(4) samples (curves b and c), the initial increase in the ammonia low-pressure adsorption is less steep than that of ZSM-5 but steeper than that of Al-Meso. The density of surface acid sites is therefore much higher in UL-ZSM-5 than in Al-Meso. For higher pressure values, the difference between these samples is more evident. For pressure values exceeding about 0.2 Torr, the rate of increase in adsorption diminishes and the isotherms become quasilinear. This linear trend may be ascribed to physisorption on surface sites and even to the formation of an adsorbate multilayer simultaneously with chemisorption [28]. After a first adsorption, ammonia was desorbed by evacuation under high vacuum at 353 K followed by a second cycle of adsorption. The irreversibly adsorbed volume can hence be determined from the difference between the adsorption volume and

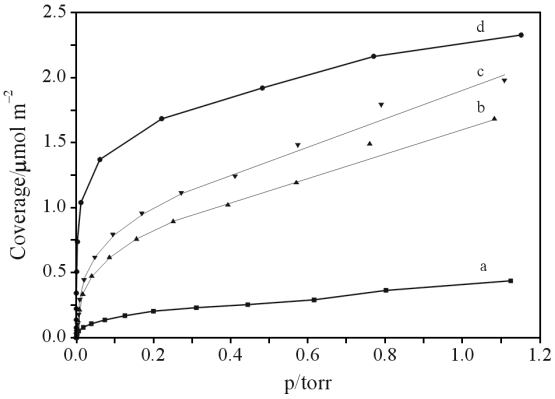

Fig. 2 Volumetric isotherms of NH_3 adsorption onto a – Al-Meso, b – UL-ZSM-5-2, c – UL-ZSM-5-4 and d – ZSM-5

Table 2 Acidity data of the aluminosilicate samples obtained by NH_3 adsorption measurements and FTIR of adsorbed pyridine

Material	NH_3 adsorption $V_{irr\ 0.2\ torr}$/μmol m^{-2}	NH_3 adsorption $V_{tot\ 0.2\ torr}$/μmol m^{-2}	FTIR pyridine Brönsted/Lewis
Al-Meso	0.07	0.21	0.5
UL-ZSM-5-2	0.14	0.82	0.6
UL-ZSM-5-4	0.26	1.02	0.8
ZSM-5	0.56	1.65	6.0

the readsorption volume at a given equilibrium pressure (plots not shown). It is believed to represent the total number of strong Brönsted and Lewis acid sites [29]. The amount of NH_3 irreversibly adsorbed at 0.2 Torr on the surface ($V_{irr\ 0.2\ torr}$) as well as the total amount of NH_3 adsorbed at the same equilibrium pressure ($V_{tot\ 0.2\ torr}$) are shown in Table 2. For the samples under study, V_{irr} markedly increases with crystallinity. For example, the value of V_{irr} is four time higher for semicrystalline UL-ZSM-5-4 than for amorphous Al-Meso (0.26 and 0.07 μmol m^{-2} respectively) but is two time lower than for crystalline ZSM-5 (0.56 μmol m^{-2}). It can be observed also that V_{tot} follows the same order as V_{irr}. Therefore, the density of surface acid sites increases in the order Al-Meso<UL-ZSM-5-2<UL-ZSM-5-4<ZSM-5.

The strength of surface acid sites can be determined on the basis of calorimetric measurements of the heats of NH_3 adsorption. The differential heat profiles as a function of coverage (adsorbed ammonia) are plotted in Fig. 3. As a general observation, in all cases, the thermal effects associated with the adsorption of NH_3 were high enough to make distinction between the two types of adsorption. Thus, a value of 70 kJ mol^{-1} for the differential heat (dotted line in Fig. 3) is generally accepted as the limit between the chemisorption and physisorption [25]. It can be observed that the initial values of the differential heats are higher than 200 kJ mol^{-1} which is probably associated with the presence of strong Lewis sites on the surface of all samples [27]. A strong decrease in the heat curves of Al-Meso (curve a) is observed with increasing NH_3 coverage. The strong decrease suggests the presence of Brönsted sites with low acid strength and indicates a heterogeneous distribution of acid strengths. However, the decrease in the heat curve is more gradual in the case of UL-ZSM-5 and ZSM-5 (curves b–d). These results clearly indicate that the strength of acid sites increases with crystallinity and follows the order: Al-Meso<UL-ZSM-5-2< UL-ZSM-5-4<ZSM-5. After covering the strong acid sites with ammonia, excepting Al-Meso, the heats curves show a plateau. Interestingly, in this region, the differential heats of ammonia adsorption reached about 30, 40 and 50–60 kJ mol^{-1} for UL-ZSM-5-2, UL-ZSM-5-4 and ZSM-5 respectively. According to literature, these values of differential heat correspond to physisorption of ammonia at the pore walls, to T–O–T bridging oxygen atoms and to terminal surface silanol groups [29]. The differences between UL-ZSM-5 and ZSM-5 materials can be explained by so-called 'confinement effect' [29, 30]. It reflects the influence of porosity on the heats of adsorption. Thus, adsorbates interact more strongly in the narrow pores than in large pores, which is in line with the high microporosity in ZSM-5 and the combined microporosity and mesoporosity in UL-ZSM-5 (Table 1). For Al-Meso, which is however a mesostruc- tured material, the acidity in this region probably arises only from hydrogen bonding interaction of ammonia to terminal silanol groups.

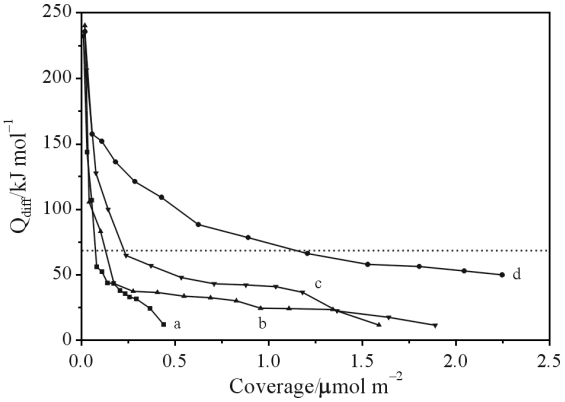

Fig. 3 Differential heat of NH_3 adsorption onto a – Al-Meso, b – UL-ZSM-5-2, c – UL- ZSM-5-4 and d – ZSM-5

While microcalorimetry allows the elaboration of a scale of acid strength, the spectroscopic techniques coupled with the adsorption of basic probe molecules yield information on the nature of acid sites. An example of FTIR spectra of adsorbed pyridine after stepwise desorption at different temperatures is presented in Fig. 4 for UL-ZSM-5-4. Bands due to hydrogen-bound pyridine (1447 and 1599 cm^{-1}), Lewis-bound pyridine (1455, 1575 and 1623 cm^{-1}), pyridine bound on Brönsted acid sites (1545 and 1640 cm^{-1}) can be observed in the spectrum recorded after desorption at 373 K (curve b) as well as a band at 1490 cm^{-1} attributed to pyridine associated with both Lewis and Brönsted acid sites [28]. It can be observed that the bands at 1447 and 1599 cm^{-1} associated with physisorbed pyridine com-

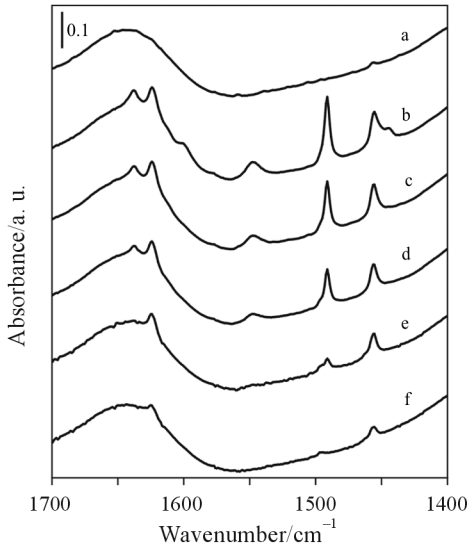

Fig. 4 FTIR spectra of UL-ZSM-5-4 sample after a – activation at 673 K and after adsorption and stepwise desorption of pyridine at b – 373, c – 423, d – 473, e – 573 and f – 673 K

pletely disappear after desorption at 423 K (curve c). The intensity of the bands corresponding to Brönsted as well as Lewis acid sites decreases as the temperature of desorption increases. After desorption at 573 K a small band at 1545 cm^{-1} is still observed for UL-ZSM-5 (curve e), whereas it lacks for Al-Meso (not shown). Therefore, the strength of Brönsted acid sites for UL-ZSM-5 materials is higher that that for Al-Meso. It must be noted that the band at 1545 cm^{-1} is observed in the IR spectrum of ZSM-5 after pyridine desorption at 673 K, indicating its highest strength of Brönsted acid sites. These results indicate

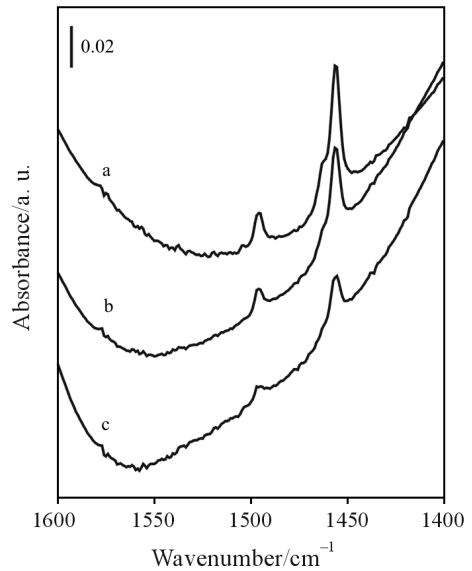

Fig. 5 FTIR spectra after adsorption and desorption of pyridine at 673 K onto a – Al-Meso, b – UL-ZSM-5-2 and c – UL-ZSM-5-4

medium-strong acid Brönsted sites on the surface of UL-ZSM-5-4 and ZSM-5 and only medium Brönsted sites on Al-Meso. This confirms that UL-ZSM-5 materials have improved Brönsted acidity when compared to the starting amorphous material. The acidity enhancement for UL-ZSM-5 may be attributed to the aluminium incorporated in tetrahedral position, in a crystalline environment similar to that of fully crystalline zeolite ZSM-5. It is thus clear that the incorporation of aluminium in a more regular environment results in the formation of Brönsted acid sites of Si–OH–Al bridging hydroxyl groups like those in ZSM-5 and having hence a medium-strong strength. On the other hand, the band at 1455 cm^{-1} corresponding to Lewis acid sites is present for all samples even after desorption at 673 K (Fig. 5). It can be observed that the IR spectrum of Al-Meso (curve a) displays a higher intensity of the band at 1455 cm^{-1} than both samples of UL-ZSM-5. Moreover, this band has a shoulder at about 1465 cm^{-1} whose intensity decreases from Al-Meso to UL-ZSM-5-4. This additional band also observed by Occelli *et al.* [28] for Al-MCM-41 was assigned to the formation at high temperature of imminium ions generated by nucleophilic attack of the framework oxygen followed by the protonation of pyridine molecules adsorbed on Lewis sites. These results are thus in conformity to ^{27}Al MAS NMR analyses that show a higher amount of extraframework aluminium atoms (responsible for the strong Lewis acidity) in Al-Meso than is UL-ZSM-5 materials. Furthermore, the calculated Brönsted/Lewis ratio (Table 2) increases with the crystallinity of the samples in the order Al-Meso< UL-ZSM-5-2<UL-ZSM-5-4<ZSM-5, in line with the above discussed results.

Conclusions

Two samples of UL-ZSM-5 having different crystallinities were prepared by solid-state crystallization starting from an amorphous mesoporous aluminosilicate. The acidic properties were monitored using different techniques and compared to amorphous and fully crystalline aluminosilicate materials. Heat flow microcalorimetry clearly indicates that the density and strength of surface acid sites are consistently improved for semicrystalline mesoporous UL-ZSM-5 when compared to amorphous mesostructured Al-Meso, while remaining lower than crystalline zeolite ZSM-5. Moreover, the Brönsted/Lewis ratio increases with crystallinity as observed by FTIR of adsorbed pyridine. This is in agreement with the higher degree of incorporation of aluminium in tetrahedral position in the crystalline framework of UL-ZSM-5, as compared to amorphous Al-Meso. However, Al-Meso shows the

highest amount of strong Lewis acid sites, which is in concordance to its highest content of aluminium in extraframework position.

The synthesis of UL-ZSM-5 materials by templated solid-state crystallization represents therefore a valuable approach to the preparation of mesoporous materials with zeolite-like characteristics and therefore with enhanced acidity in comparison with the mesostructured aluminosilicate precursor.

References

1 D. Trong On and S. Kaliaguine, 'Zeolite/mesoporous molecular sieves composite materials' in Nanoporous Materials-Science and Engineering, G. Q. Lu and X. S. Zhao Eds., Imperial College Press, London 2004.
2 Y. Liu and T. J. Pinnavaia, J. Mater. Chem., 12 (2002) 3179.
3 D. Trong On, D. Giscard, C. Danumah and S. Kaliaguine, Appl. Catal. A: General, 222 (2001) 299.
4 K. R. Kloetstra, H. van Bekkum and J. C. Jansen, Chem. Commun., (1997) 2281.
5 A. Karlsson, M. Stocker and R. Schmidt, Microporous Mesoporous Mater., 27 (1999) 181.
6 L. Huang, W. Guo, P. Deng, Z. Xue and Q. Li, J. Phys. Chem. B, 104 (2000) 2817.
7 Y. Liu, W. Zhang and T. J. Pinnavaia, J. Am. Chem. Soc., 122 (2000) 8791.
8 Y. Liu, W. Zhang and T. J. Pinnavaia, Angew. Chem. Int. Ed., 40 (2001) 1255.
9 Y. Liu and T. J. Pinnavaia, Chem. Mater., 14 (2002) 3.
10 Z. Zhang, Y. Han, L. Zhu, R. Wang, Y. Yu, S. Qiu, D. Zhao and F-S. Xiao, Angew. Chem. Int. Ed., 40 (2001) 1258.
11 Y. Han, S. Wu, Y. Sun, D. Li, F.S. Xiao, J. Liu and X. Zhang, Chem. Mater., 14 (2002) 1144.
12 A. Sakthivel, S. J. Huang, W. H. Chen, Z. H. Lan, K. H. Chen, T. W. Kim, R. Ryoo, A. S. T. Chiang and S. B. Liu, Chem. Mater., 16 (2004) 3168.
13 D. Trong On and S. Kaliaguine, Angew. Chem. Int. Ed., 41 (2002) 1036.
14 D. Trong On and S. Kaliaguine, J. Am. Chem. Soc., 125 (2003) 618.
15 D. Trong On, A. Ungureanu and S. Kaliaguine, Phys. Chem. Chem. Phys., (2003) 3534.
16 D. Trong On, A. Nossov, M. A. Springuel Huet, C. Schneider, J. L. Bretherton, C. A. Fyfe and S. Kaliaguine, J. Am. Chem. Soc., 126 (2004) 14325.
17 D. Trong On and S. Kaliaguine, Angew. Chem. Int. Ed., 40 (2001) 3248.
18 V. T. Hoang, D. Trong On and S. Kaliaguine, Stud. Surf. Sci. Catal., 146 (2003) 145.
19 P. Yang, D. Zhao, D. I. Margolese, B. F. Chmelka and G. D. Stucky, Nature, 396 (1998) 152.
20 D. Trong On, M. P. Kapoor, E. Thibault, J. E. Gallot, G. Lemay and S. Kaliaguine, Microporous Mesoporous Mater., 20 (1998) 107.
21 C. A. Emeis, J. Catal., 141 (1993) 347.
22 R. B. Borade and A. Clearfield, Catal. Lett., 31 (1995) 267.
23 K. R. Kloetstra, H. W. Zandbergen and H. van Bekkum, Catal. Lett., 33 (1995) 157.
24 X. Chen, L. Huang, G. Ding and Q. Li, Catal. Lett., 44 (1997) 123.
25 A. Auroux, Top. Catal., 4 (1997) 71.
26 A. Auroux, Top. Catal., 19 (2002) 205.
27 M. J. Meziani, J. Zajac, D. J. Jones, S. Partyka, J. Roziè re and A. Auroux, Langmuir, 16 (2000) 2262.
28 M. L. Occelli, S. Biz, A. Auroux and G. J. Ray, Microporous Mesoporous Mater., 26 (1998) 193.
29 Kosslick, H. Landmesser and R. Fricke, J. Chem. Soc., Faraday Trans., 93 (1997) 1849.
30 E. G. Derouane, Zeolites, 13 (1993) 67.

Received: September 20, 2006
Accepted: November 24, 2006

DOI: 10.1007/s10973-006-6891-0